Received: 1 November 2016 | Revised: 28 June 2017 | Accepted: 29 June 2017

DOI: 10.1002/gj.2992

WILEY

RESEARCH ARTICLE

Quaternary tectonostratigraphic evolution of the Vlora Basin, south-western Albania

Giuseppe Palladino[1] | Paolo Giannandrea[2] | Agata Siniscalchi[3] | Cosimo Magri'[3] | Francesco Loiacono[3]

[1] Department of Geology and Petroleum Geology, School of Geosciences, University of Aberdeen, Aberdeen, UK

[2] Dipartimento di Scienze, Università degli Studi della Basilicata, Campus Macchia Romana, Potenza, Italy

[3] Dipartimento di Scienze della Terra e Geoambientali, Università di Bari Aldo Moro, Bari, Italy

Correspondence
Giuseppe Palladino, Department of Geology and Petroleum Geology, School of Geosciences, University of Aberdeen, Old Aberdeen Campus, Aberdeen AB24 3FX, UK.
Email: giuseppe.palladino@abdn.ac.uk

Funding information
Fondi di Ateneo RIL 2011, 2013 (Universita' degli Studi della Basilicata); CISM Project

Handling Editor: S. Tyrrell

The Vlora Bay is a roughly north-west–south-east-oriented tectonic depression located at the collision zone between the Apulian Foreland and the Albano-Hellenic Chain in south-western Albania. The bay exhibits a triangular-shaped geometry, which is the result of different tectonic phases that occurred mostly between the end of the Neogene and the Quaternary. The bay consists of two distinct physiographic sections: a shallow water marine offshore area and a recently emerged onshore sector. Along the onshore sector, Pleistocene clastic sediments filling the Pleistocene Vlora Basin crop out due to the recent uplift phases. The sedimentological and stratigraphic organization of the Vlora Basin deposits and the role played by Quaternary tectonic structures in their deposition are the main topics of this paper. A detailed field survey, supported by a geoelectrical survey, reveals a series of unconformity-bounded stratigraphic units deposited in two north-west–south-east-oriented subbasins. The two subbasins are separated by an intrabasinal, fault-bounded, pre-Quaternary morpho-structural high and are mainly filled by shallow marine to continental deposits. A detailed structural analysis shows different tectonic phases affecting the area during the Pleistocene. Additionally, the geophysical survey facilitates the reconstruction of the deep structure of the basin and provides a better definition of the basin margins. Based on both geological and geophysical data, a tectonostratigraphic evolutionary model is proposed for the Vlora Basin Pleistocene sedimentary infill. This model consists of three phases of sedimentation that were essentially controlled by fault activity and by the progressive uplift of the area.

KEYWORDS

Quaternary palaeogeography, south-western Albania, tectonics and sedimentation, unconformity-bounded stratigraphic units, Vlora Basin

1 | INTRODUCTION

In the southern sector of the peri-Adriatic region, the orogens resulted mainly from the deformation of different Mesozoic–Cenozoic palaeodomains and the subduction of the Apulian Plate during the Neogene (Aliaj, 1987, 2006; Bosellini, 2002; Channel, D'Argenio, & Horvath, 1979; D'Agostino et al., 2008; Dercourt, Ricou, & Vrielynck, 1993; Dercourt, Zonenshain, Ricou, et al., 1986; Jouanne et al., 2012; Papa & Kondo, 1968; Pinter, Grenerczy, Weber, Stein, & Medak, 2006; Figure 1a). A common characteristic observed in these mountain chains (i.e., the Albanides and the Southern Apennines) is that during the Quaternary, the front–foredeep–foreland system underwent a general uplift that was accommodated by extensional and strike–slip tectonic structures (Doglioni, Mongelli, & Pieri, 1994). This process led to the local emergence of the foreland area and the progressive shallowing of the foredeep areas, which were filled with molasse deposits (i.e., the Peri-Adriatic Depression or Bradanic Trough). In this geodynamic context, space for sediment accommodation may remain available in a series of small, fault-controlled basins characterized by shallow water to continental sediment deposition (Giannandrea, 2009; Palladino, 2011). In the western sector of the external Albano-Hellenic Chain, the Vlora Basin provides a good example (Loiacono, De Marco, Dicoladonato, Gadaleta, & Durmischi, 2011; Figure 1b). The Vlora Basin is a narrow, north-west–south-east-trending, 20-km-long, triangular-shaped sedimentary basin extending roughly parallel to the south-eastern margin of the Adriatic Sea. It consists of a young tectonic depression filled by Quaternary continental to marine deposits, which rest unconformably on a deformed Neogene marine

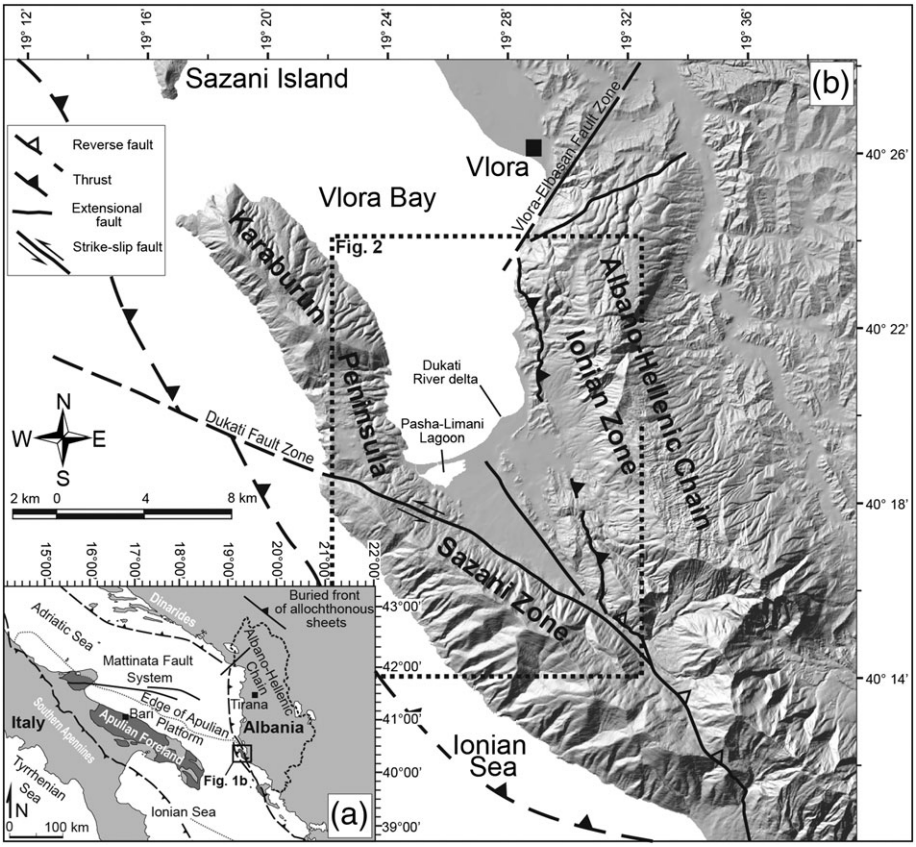

FIGURE 1 (a) Geological sketch map of the southern peri-Adriatic region. The Apulian Platform represents the foreland/forebulge sector shared by both the southern Apennines and the Hellenic–Albanides fold-and-thrust belts. (b) Digital Terrain Model (DTM) of the Vlora Bay area showing the main tectonostratigraphic domains and the location of the Figure 2 (dashed box)

succession pertaining to the Peri-Adriatic Depression, and Mesozoic deposits belonging to the Sazani and Ionian palaeodomains (ISPGJ-IGJN, 1982; ISPGJ-IGJN, 1983). The basin borders are represented by the steep, fault-controlled relief of the carbonate Karaburun Peninsula and Sazani Island to the south-west, the Albano-Hellenic Chain to the east, and the Vlora-Elbasan lineament to the north-west. The Vlora Basin can be subdivided into two distinct sectors that exhibit very different features: (a) The north-western sector consists of a shallow water marine area characterized by active sedimentation (Loiacono et al., 2008; Loiacono et al., 2011; Savini et al., 2011), and (b) the south-eastern sector consists of a recently emerged area subjected to uplift and active fluvial erosion (Carcaillet, Mugnier, Koçi, & Jouanne, 2009; Figure 1b).

Our attention is mainly focused on the latter sector where Pleistocene continental to shallow marine sediments crop out, filling two distinct depocentres; in this paper, these are labelled as the Tragjas and Dukati subbasins (Figures 2 and 3). The recognized subbasins are separated by the flat-topped Orikum Ridge, which consists of a pre-Quaternary bedrock structural high.

To reconstruct the Pleistocene stratigraphic sequence and understand the relationships occurring between Quaternary tectonics and sedimentation in the Vlora Basin, detailed geological and geophysical surveys were conducted in an area approximately 100 km^2 wide and located 15 km south of the city of Vlora. The geological survey enabled us to characterize different depositional environments, which have been grouped into five main facies associations, and identify three stratigraphic units bounded by unconformities. A large quantity of structural data was collected along the major tectonic lineaments to establish the role played by tectonics in controlling the differential accommodation space of the subbasins.

Finally, three electrical resistivity tomographies (ERTs) were obtained to delineate the geometry of the basin margins, the main facies changes, and the occurrence of tectonic lineaments and stratigraphic unit boundaries in the subsurface of the Dukati subbasin.

2 | GEOLOGICAL SETTING

The Vlora Basin is located at the front of the External Albanides (Figure 2). The Albano-Hellenic Chain was derived from the deformation of Mesozoic palaeogeographic structural highs and lows, namely, from east to west, the Krasta–Cukali, Kruja, Ionian, and Sazani zones (Argnani, 2013; Meço & Aliaj, 2000; Robertson & Shallo, 2000; Velaj, Davinson, Serjani, & Alsop, 1999). Horst and graben-like palaeogeographic elements resulted from the extensional tectonic phases occurring during the Late Jurassic to Middle Cretaceous (Gealey, 1988). Structural highs consisting of carbonate platforms and shelves (Kruja and Sazani zones) connected to the adjacent deep basins (corresponding to the Ionian Zone) through a series of steeply inclined ramps and slopes.

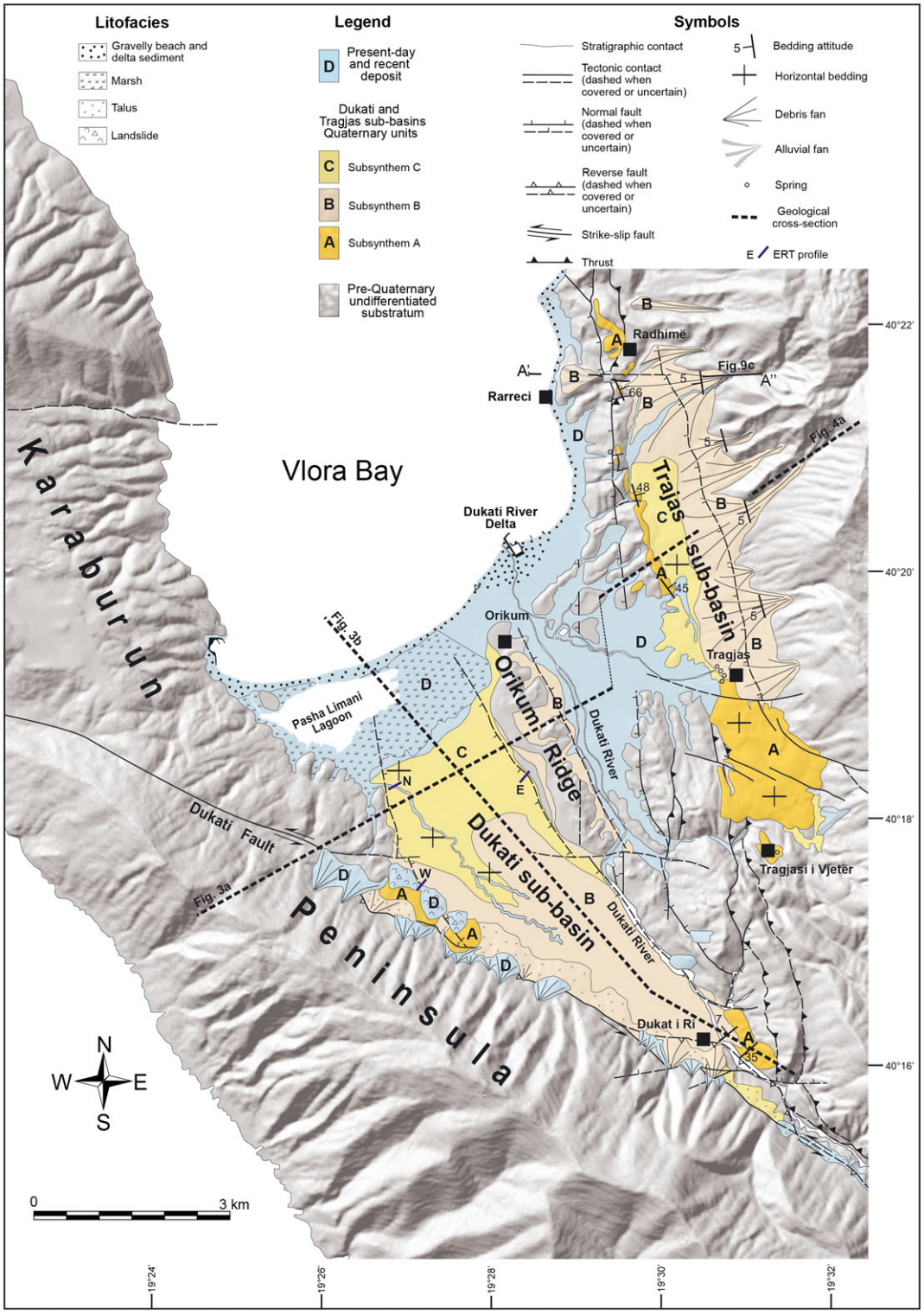

FIGURE 2 Geological map of the Vlora Basin showing the recognized Quaternary units, the undifferentiated pre-Quaternary substratum, and the main tectonic structures. The main physiographic units of the Vlora Basin, represented by the Dukati and Tragjas subbasins and the Orikum Ridge, are also included. A DTM is used as a base for the map [Colour figure can be viewed at wileyonlinelibrary.com]

The north-eastern margin of the Vlora Basin corresponds to the Cika–Tragjasi belt, the most external tectonic unit of the Ionian Basin Zone. The south-western margin coincides with the Mesozoic carbonates of the Karaburun Peninsula and Sazani Island (KCUs), which are part of the Sazani Zone foreland area. The basin bottom consists of different stratigraphic units relating to the Peri-Adriatic Depression foredeep. The Vlora–Elbasan lineament roughly delineates the northern boundaries of the basin (Roure et al., 2004).

The Ionian Basin deposits mainly consist of Mesozoic carbonates followed upward by Meso-Cenozoic deepwater deposits. They are organized in a series of stacked west–south-west-facing allochthonous sheets detached along Triassic evaporites.

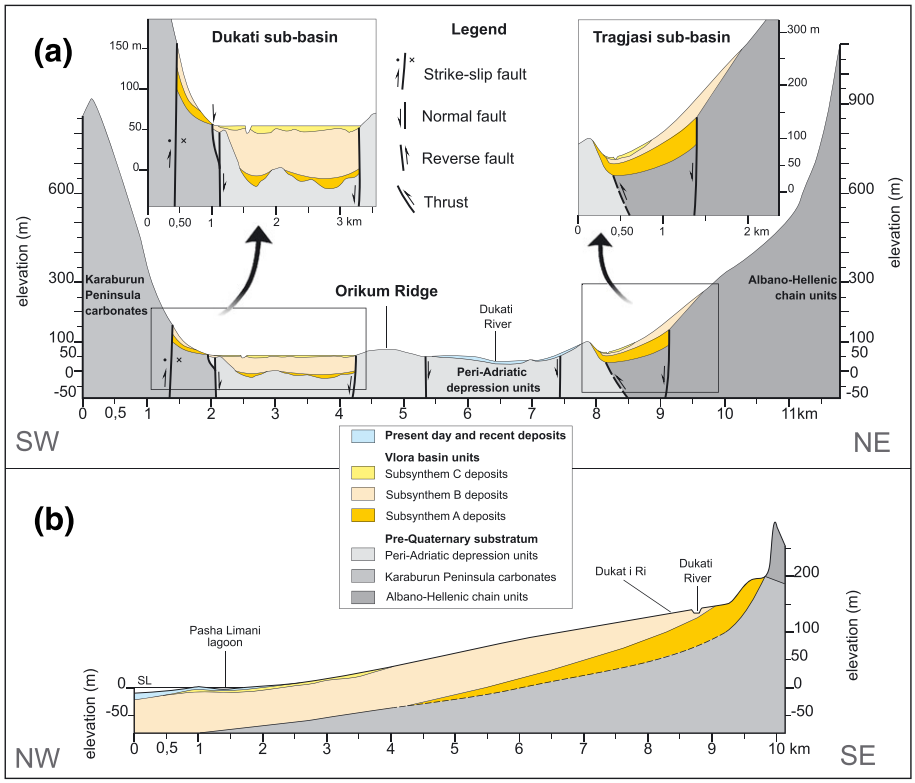

FIGURE 3 (a) Transversal and (b) longitudinal geological cross-sections through the Tragjas and Dukati subbasins (see cross-sectional traces in the Figure 2). In colour the recognized Quaternary units. Different greyscale tonalities are utilized for the pre-Quaternary substratum. Vertical scale exaggerations are performed in order to emphasize the thickness variations of the recognized stratigraphic units [Colour figure can be viewed at wileyonlinelibrary.com]

The Sazani Zone deposits consist mostly of a thick Mesozoic succession comprising Triassic and Jurassic dolomites overlain by Cretaceous to Oligocene shallow marine limestones (ISPGJ-IGJN, 1982; ISPGJ-IGJN, 1983).

The Peri-Adriatic Depression deposits (PDUs) consist of a thickening-and coarsening-upward sequence of Cenozoic flysches and molasses.

The External Albanides primarily developed during the Late Oligocene–Miocene, after the deformation of the south-western side of the Vardar Ocean passive margin (Frasheri, Nishani, Bushati, & Hyseni, 1996; Lacombe, Malandain, Vilasi, Amrouch, & Roure, 2009; Roure, Prenjasi, & Xhafa, 1995; Sejdini, Constantinescu, & Piperi, 1994; Velaj et al., 1999). The Neogene compressional tectonic phases caused the progressive overthrusting of the Ionian Zone onto the Sazani platform carbonates at the Miocene–Pliocene boundary (ISPGJ-IGJN, 1982; ISPGJ-IGJN, 1983; Speranza, Islami, Kissel, & Hyseni, 1995). According to Roure (2008), because of rheology contrasts between the Sazani Zone platform carbonates and finely bedded Ionian Zone basinal deposits, a triangle zone structural style was developed in the Vlora area. The growth of this structure led to the progressive uplift of the Karaburun–Sazani carbonate blocks and the partial emergence of the Vlora Bay area. Currently, the tectonic evolution of the Vlora Bay area is related to contractional and transcurrent tectonics (Jouanne et al., 2012). In particular, major thrusts and strike–slip lineaments (i.e., the Vlora–Elbasan Fault) control the sedimentary infill and the tectonic style in the External Albanides.

3 | METHODS

To reconstruct the Quaternary tectonostratigraphic evolution of the Vlora Basin, an interdisciplinary study encompassing sedimentology, stratigraphy, structural geology, and geophysics was undertaken. To this end, geological and geophysical surveys were conducted along the emerged south-eastern sector of the bay, including the villages of Radhimë and Dukati i Ri.

The stratigraphic subdivision of the recognized Quaternary deposits is based on the concept of unconformity-bounded stratigraphic units (Chang, 1975; Giannandrea, Marino, Romeo, & Schiattarella, 2014; Salvador, 1987, 1994). According to this method, each stratigraphic unit coincides with a layered body of sedimentary rocks confined between two map-scale discontinuities. A series of structural data have been collected from suitable key outcrops to better understand the role played by Quaternary tectonics in the sedimentation in the Vlora Basin. The structures essentially consist of fault planes containing well-preserved kinematic indicators. Fault planes and related slickensides were drawn as great circles and poles, respectively, on equal-area lower hemisphere stereoplots using STEREONET 9 by Allmendinger (http://www.geo.cornell.edu/geology/faculty/RWA/).

The geophysical survey consisted of acquiring three ERTs for the geometric characterization of the geological bodies in the subsurface. The ERT measurements were collected using a computer-controlled system with 48 electrodes laid out in a straight line (235 m) with a

minimum spacing of 5 m. During the geoelectrical survey, a multielectrode system (Syscal R2, Iris Instruments) was used for data acquisition. Three arrays were selected for each measurement: dipole–dipole arrays because of their good lateral resolution, Wenner–Schlumberger arrays because of their vertical resolution, and pole–pole arrays that provide the widest horizontal coverage and deepest penetration. The entire datasets were inverted both separately and jointly with RES2DINV (Loke & Barker, 1996) to obtain a subsurface image of the electrical resistivity pattern. Topography was included in the inversion. The two-dimensional inversion routine applies a Gauss–Newton least squares method (Loke & Barker, 1996) based on a finite-difference model of the subsurface, automatically adjusted in an iterative process that reduces the sum of the squared residuals between the measured and calculated apparent resistivities.

4 | FACIES ASSOCIATIONS AND STRATIGRAPHY OF THE VLORA BASIN DEPOSITS

The following study is based on a detailed field survey that produced the geological map shown in Figure 2. The Vlora Basin is subdivided into two adjacent depocentres, namely, the Dukati and Tragjas subbasins, which have similar ages but slightly different sedimentological characteristics (Figure 3). The two areas of sedimentation are separated by a flat-topped, high-relief area that is referred to as the Orikum Ridge and consists of Neogene rocks belonging to the Peri-Adriatic Depression basin fill, which uplifted during the Middle Pleistocene. The stratigraphic analyses are mainly conducted by recognizing surfaces with different discontinuities. Facies variations, lithological contacts, and geometrical relationships are used to recognize the different stratigraphic units. The detailed sedimentological analyses, which took into account the grain size, sedimentary structures, and trace fossils, allow us to recognize a series of gravelly and sandy facies (Table 1). These facies are grouped into five facies associations (Figure 4; Table 2).

4.1 | Dukati subbasin

The Dukati subbasin deposits are discontinuously observable between Dukati i Ri village and Pasha-Limani Lagoon (Figure 2). The subbasin shows a deactivated, slightly seaward-dipping planar top (Figure 3a,b) that is deeply incised by the Dukati River and several secondary rills converging towards Pasha-Limani Lagoon. Within the Dukati subbasin, four facies associations can be distinguished and are named F1, F3, F4, and F5 (Table 2).

4.1.1 | Dukati subbasin facies associations

Facies association F1 (Figure 4).primarily consists of conglomerates cropping out near Dukati i Ri village (Table 2). Facies Gcm consists of

TABLE 1 Vlora Basin sedimentary facies

Facies codes	Description	Interpretation
Bc	Poorly sorted clast-supported breccias. Angular clasts ranges in size from 1 to 50 cm.	Breccias accumulated by rock fall mechanisms.
Bcm	Poorly to moderately sorted clast- to matrix-supported breccias. Angular clasts ranging in size from 1 to 20 cm. Matrix, locally abundant, consists of fine-grained sand or red/light grey clay.	Debris flow deposits (cohesive debris flows; Sanders et al., 2009).
Bcc	Lens-shaped clast-supported breccias made by angular and subordinately subrounded clasts. Clast sizes range from 1 to 6 cm. The matrix consists of coarse to fine sand. Distinctive character is the reverse gradation.	Deposits from stream-driven, high-density gravelly traction carpets (Todd, 1989).
Gcm	Crudely bedded poorly to moderately sorted clast-supported conglomerates. Clast may vary from subangular to rounded, their sizes range from 1–2 cm to 40–50 cm. Occurrence of marked erosional basal surface.	Debris flows associated to turbulent flows, inertial flows (Miall, 1996), or to hyperconcentrated flows (Pierson, 1980; Smith, 1986).
Gch	Horizontally bedded clast-supported gravel. Bed thickness varies from few centimetres to some decimetres. Clast sizes vary from some centimetre to 60 cm.	Sheetfloods, longitudinal bars (Miall, 1996).
Gcp	Clast-supported gravel with planar cross-stratification. The well-rounded clasts ranges in sizes from 1 to 10 cm. Layer thickness ranges from 40 to ~150 cm. Cross-bedding attitudes vary from 7° to 40°. Occasional imbrications.	Frontal and lateral accretion of gravelly bars (Miall, 1992).
Gct	Well-rounded clast-supported gravel with trough cross-stratification. Layer thickness is ~100 cm. Clast sizes ranges from some centimetre to 10 cm.	Streamflow deposits (Miall, 1992).
SGh	Structureless or horizontally bedded matrix-supported gravel with reddish sandstone matrix. Angular to subrounded clast varying in size from 1 to 3 cm. Bed thickness varies from 5 to 40 cm.	Sheetflood deposits (Blair, 1987; Blair & McPherson, 1994), with bedload pulsation (Reid & Frostick, 1984).
Sm	Medium- to fine-grained structureless sand. Layer thickness range from 10 to 50 cm. Locally occurrence of marine trace fossils.	Deposits from rapid suspension fallout from highly concentrated turbulent flows (Smith, 1986).
SMh	Horizontally bedded alternation of sand, silt, and mudstones. Local bioturbations.	Decantation from overbank flood (Besley & Turner, 1983; Miall, 1996; Van Houten, 1968; Walker, 1967).
SMb	Medium- to fine-grained structureless sand with rare to abundant biotubations. Bed thickness vary from 20 to 100 cm.	Rapid suspension fallout from highly concentrated turbulent flows.
P	Brown to red silty sand with rare to abundant occurrence of pebbles and traces of roots.	Palaeosol (Mack & Madoff, 2005).

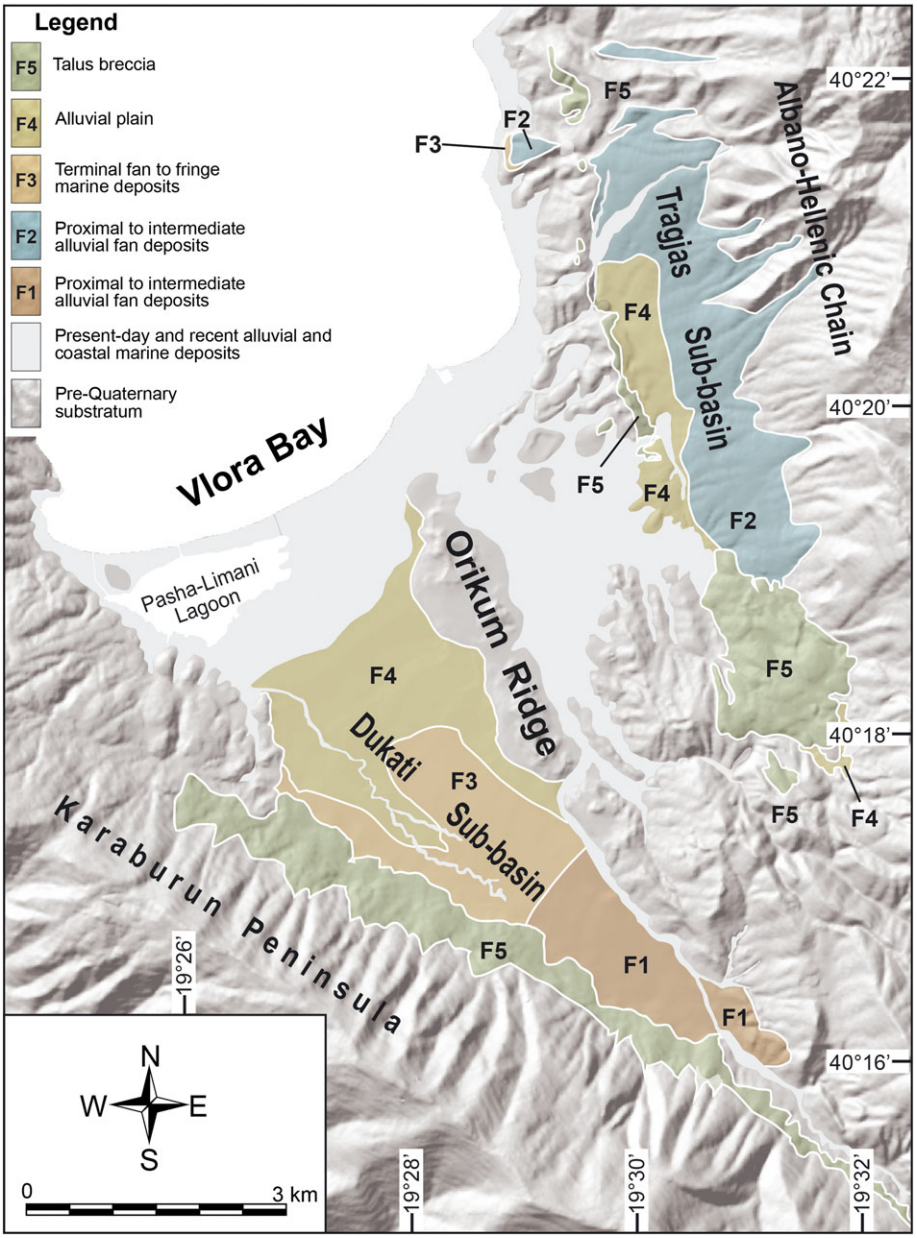

FIGURE 4 DTM of the Vlora Bay showing the distribution of the main facies associations recognized in the Dukati and Tragjas subbasins [Colour figure can be viewed at wileyonlinelibrary.com]

TABLE 2 Vlora Basin facies associations

Facies association	Dominant facies	Spatial distribution	Environmental interpretation
F1	Gcm, Gch, and Gcp, with minor Sm	Gcm/Gch ratio varies laterally in the direction of the transport from >1 to <1. Facies Gcp only occur in the intermediate settings.	Proximal to intermediate sector of an alluvial fan
F2	Bcc and Bcm	Bcc and Bcm commonly alternate in equal proportions. Bed thickness decreases from the apex towards the intermediate sectors.	Proximal to intermediate sector of a debris-flow dominated alluvial fan
F3	Gcp, Gct, SMb, and SMh with minor Gch, Gcm, and Sm	Conglomerate facies (Gcp and Gct with minor Gch, Gcm, and Sm) commonly prograde over sandy facies giving rise to a coarsening upward sequence. Sandy facies (SMb and SMh with bioturbation) increase down-current, and conglomerate facies became thinner and isolated	Terminal stream dominated fan to fan fringe marine
F4	Gch, Gcp, and Gct, with minor Sm, SMh, SGh, and P	Tabular-shaped conglomerates bounded by basal erosional surfaces alternating with minor sand bodies.	Alluvial plain
F5	Bc and minor Bcm	Bc and Bcm alternate in equal proportions forming amalgamated crudely bedded sequences.	Talus slope breccia

crudely bedded, clast-supported, poorly to moderately sorted, lens-shaped conglomerates (Figure 5a). Clasts vary in shape from angular to rounded, and clast sizes range from 1–2 cm to 40–50 cm. A sandy matrix is common. These conglomerate bodies are commonly structureless and show a marked erosional base. Facies Gch consists of centimetre- to decimetre-thick, horizontally bedded, tabular-shaped, clast-supported gravels (Figure 5b). Clasts vary in shape from angular to rounded and may range in size from a few centimetres to 60 cm. Facies Gcp consists of clast-supported gravel beds showing planar cross-bedding. Bed attitudes vary from 7° to 40° (Figure 5a). Layer thicknesses may range from 40 to 150 cm. Clasts, which range in size from 1 to 10 cm, are well rounded and show occasional imbrication. Facies Sm consists of medium- to fine-grained structureless sandstone (Figure 5c), and the layer thickness varies from 10 to 50 cm. Facies association F1 is attributed to the proximal and intermediate sectors of an alluvial fan dominated by debris flow processes (Blair & McPherson, 1994; Gloppen & Steel, 1981; Table 2). The distinction between the proximal and intermediate sectors of the considered alluvial fan is determined by studying the Gcm, Gch, and Gcp relative abundances in the conglomerate facies. In the proximal sector (near Dukati i Ri village), facies Gcm prevails over Gch, whereas Gcp is absent. In the intermediate sector, facies Gch prevails over facies Gcm, and facies Gcp is present. Facies Sm is commonly identified in both sectors.

Facies association F3 (Figure 4) crops out in the central portion of the Dukati subbasin and consists of different facies. Facies Gct consists of lens-shaped clast-supported gravels showing trough cross-stratification (Figure 5b). The layer thickness is generally approximately 100 cm. Clasts are well-rounded and range in size from a few centimetre to 10 cm. Facies SMh consists of horizontally bedded, fine-grained sandstone layers alternating with siltstone and mudstone. Bioturbation in the sandstone may be locally abundant (Figure 5c,d). Facies SMb consists of medium- to fine-grained structureless sandstone with rare bioturbation. The layer thickness may vary from 20

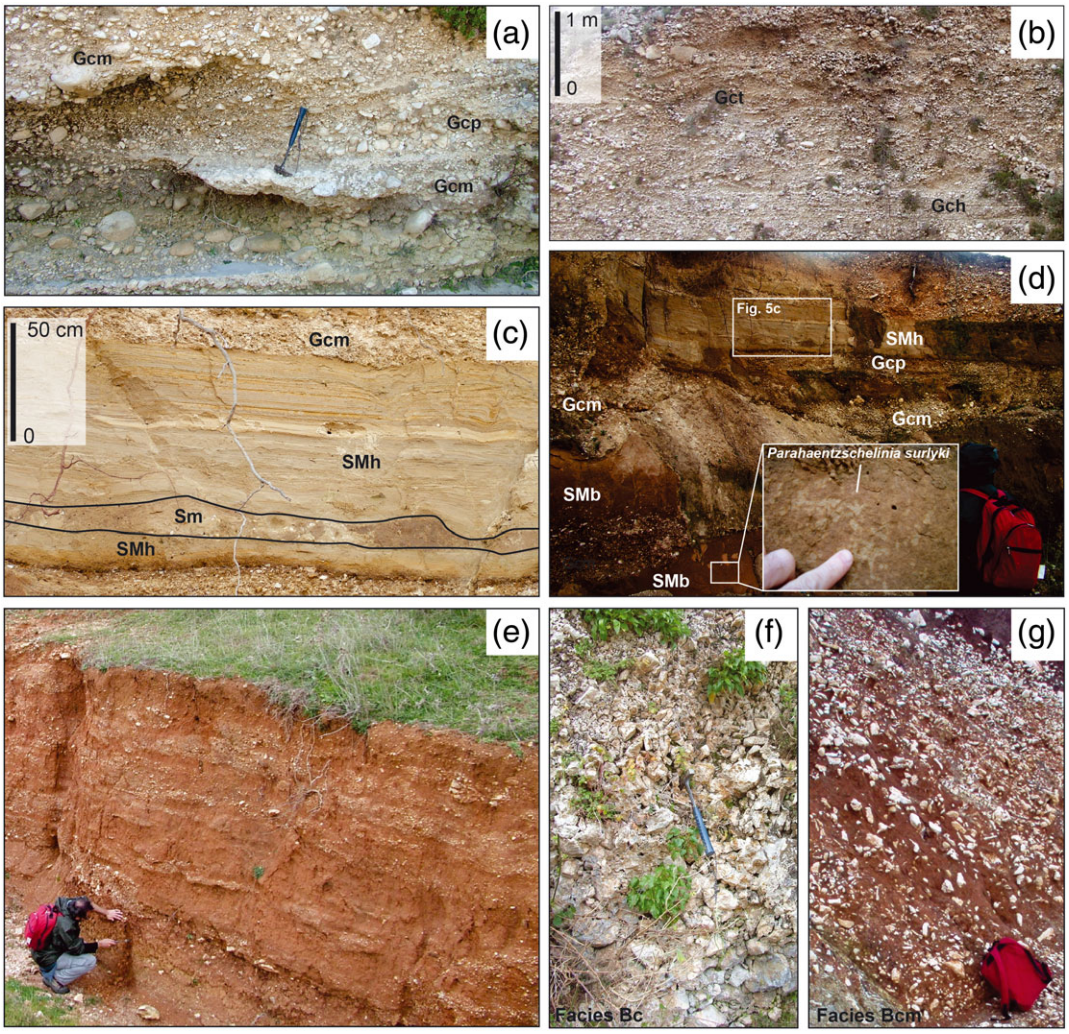

FIGURE 5 Vlora Basin facies associations: (a) and (b) Photographs showing the main characters of facies association F1. Alternating structureless and cross-bedded conglomerates belonging to facies Gcp, Gct, and Gcm are showed. The occurrence of isolated big-sized clasts in the deposit denotes their close proximity to the source area; (c) and (d) photographs showing the main characters of facies association F3. This facies association consists of alternating marine sandy lithologies, represented by Sm, Smb, and Smh facies, and conglomerates. Among these latter, Gcm and Gcp are the most commonly recognized facies. The occurrence in the facies SMb of trace fossils, such as *Parahaentzschelinia surlyki* (in the box), allowed the attribution of this facies to a beach environment; (e) photograph showing the main characters of facies association F4. The facies association consists of sporadic conglomerates alternating with reddish palaeosoil; and (f) photographs showing the main characters of facies association F5. The two main facies, Bc and Bcm, are showed [Colour figure can be viewed at wileyonlinelibrary.com]

to 100 cm (Figure 5d). Facies Gcp, which was described in the previous facies association, is also common. Facies association F3 is attributed to a terminal fan to fan fringe marine environment dominated by stream flows (Gloppen & Steel, 1981; Table 2). The occurrence in the facies SMb of trace fossils, such as *Parahaentzschelinia surlyki* (Figure 5d), allows us to relate the facies to a beach environment (Fürsich, Wilmsen, & Seyed-Emami, 2006) characterized by short periods of increased water energy (Dam, 1990). Facies SMb is associated with the rapid deposition of highly concentrated turbulent flows. In this sector, the lens-shaped conglomerates (Facies Gct) are interpreted as filled distributary channels. Facies SMh is interpreted as overbank and/or restricted lagoon/small coastal lake deposits (similar to the present-day Pasha-Limani Lagoon).

Facies association F4 (Figure 4) includes facies Gch, Gcp, and Gct, with minor Sm, SMh, SGh, and P. Facies SGh consists of structureless or horizontally bedded matrix-supported gravels (Figure 5e), where the matrix consists of reddish sands. Clasts vary in shape from angular to subrounded and range in size from 1 to 3 cm. Gravel beds show a lens-shaped geometry and may vary in thickness from 5 to 40 cm. Facies P consists of brown- to red-coloured silty sandstone (Figure 5e). Locally, pebble layers and traces of roots occur. This facies is interpreted as a palaeosoil. Facies association F4 is attributed to an alluvial plain environment mainly dominated by braided stream processes (Miall, 1992, 1996; Table 2).

Facies association F5 (Figure 4) crops out along the south-west border of the basin at the base of the Karaburun Peninsula slope. It consists of two prevailing facies, namely, Bc and Bcm (Table 1). Facies Bc consists of poorly sorted clast-supported breccias comprising angular clasts (Figure 5f). The clast size ranges from 1 to 50 cm. The clasts are derived from the local carbonate rock substrate, and the matrix is generally absent. Bcm consists of poorly to moderately sorted, clast- to matrix-supported breccias with angular clasts (Figure 5g). Clast size ranges from 1 to 20 cm, and similar to the previous facies, the clasts are derived from the local carbonate bedrock. The matrix, which is red or light grey in colour, varies from abundant to scarce. The facies association F5 deposits are interpreted as talus slope breccias deposited along a slope by rock-fall mechanisms and subordinately from cohesive debris flows (Paschinger, 1950; Penck, 1921; Sanders, Ostermann, & Kramers, 2009, 2010; Table 2).

4.2 | Tragjas subbasin

The Tragjas subbasin deposits crop out widely between Radhimë and Tragjas villages (Figure 2). These deposits unconformably overlie the Ionian Zone thrust sheets (Figure 1). The stratigraphic succession is well exposed within a series of incised gullies.

4.2.1 | Tragjas subbasin facies associations

The Tragjas subbasin infill consists of three main facies associations (Table 2). F2, F4, and F5. Facies associations F4 and F5 show the same characteristics as those described for the Dukati subbasin; however, they differ in clast composition. In fact, this portion of the Vlora Basin is mainly fed by the Ionian units, and the clasts mostly consist of cherty limestone, calcarenite, and sandstones. Facies association F2 (Figure 4) mainly consists of lens-shaped breccias, similar to facies Bcm and Bcc (Table 1). Facies Bcm has been previously described. Facies Bcc consists of lens-shaped, clast-supported, angular and subordinately subrounded breccias. The clast sizes vary from 1 to 6 cm (Figure 6a, b). Breccia bodies are commonly 60 cm thick and often show a reverse gradation (Figure 6b) and strata dips of 10°–20°. This facies is attributed to stream-driven, high-density gravelly traction carpets (Todd, 1989) with subordinate cohesive debris flows (Paschinger, 1950; Penck, 1921; Sanders et al., 2009; Table 2). Facies association F2 is attributed to proximal-intermediate debris flow-dominated alluvial fans.

4.3 | Vlora Basin stratigraphy

The sediments filling the Vlora Basin are stratigraphically included between the deformed Meso-Cenozoic bedrock (represented by the Karaburun, Peri-Adriatic, and Albano-Hellenic units) and the Holocene Vlora Bay deposits (consisting of alluvial, marsh, beach, and delta

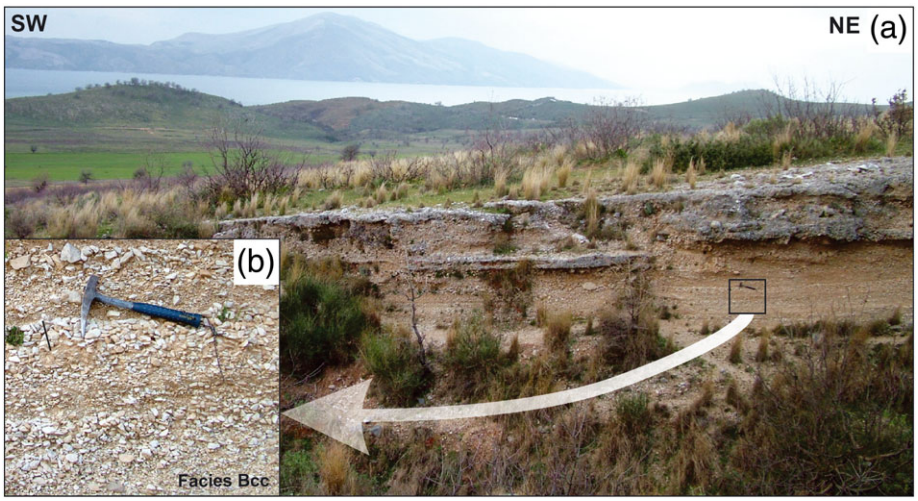

FIGURE 6 Vlora Basin facies associations: Photographs showing the main characters of facies association F2 observable SW of the Radhimë village. (a) Natural cross-section of a debris flow-dominated alluvial fan showing lens-shaped breccias referred to the facies Bcm and Bcc; (b) detail of the previous photograph showing a breccia body with reverse gradation [Colour figure can be viewed at wileyonlinelibrary.com]

sediments; ISPGJ-IGJN, 1982; ISPGJ-IGJN, 1983; Loiacono et al., 2011; Savini et al., 2011). Their chronostratigraphic attribution, which is difficult to obtain because of the lack of key fossil associations and marker layers, can be broadly deduced by correlating the study units with similar formations cropping out along the peri-Adriatic region (Figure 7). It encompasses the whole Pleistocene. At the base of the Vlora Basin succession, a major unconformity (S1) reveals the tectonic and uplift stages leading to the emersion of the pre-Quaternary substratum at the end of Pliocene. This surface is easily recognizable in the subsurface (see the next sections). The identification in the Pleistocene succession of two minor unconformities, which are recognizable at the Vlora Basin scale, allows us to subdivide the successions into three subsynthems according to unconformity-bounded stratigraphic unit nomenclature (Chang, 1975; Salvador, 1994) that are referred to as Subsynthems A, B, and C (Figure 7). The erosional surface separating Subsynthems A and B (S2) is an angular unconformity showing a clear erosive truncation (Figure 8a), which, in the Dukati subbasin sandy facies, passes seaward to a paraconformity. The surface separating Subsynthems B and C (S3; Figure 8b) is a disconformity. The newly recognized stratigraphic units will be described in the following sections.

4.3.1 | Subsynthem A

Subsynthem A includes sediments pertaining to the facies association F5, which mainly consists of fan-shaped talus breccia abundantly deposited on both sides of the Vlora Basin (Figure 7). Laterally associated sandy, silty, and clayey deposits, recognized in the subsurface, are interpreted as the distal counterpart of Subsynthem A (see the next sections). The thickness may laterally vary from a few metres to some tens of metres. Along the south-western side, coinciding with the Dukati subbasin, basal unconformity S1 cuts through the Mesozoic Sazani limestones and the Peri-Adriatic Depression siliciclastic deposits. Along the north-eastern side, which corresponds to the Tragjas subbasin, the S1 surface cuts into the Ionian Basin deepwater limestones and the Peri-Adriatic Depression siliciclastic deposits. In the first area, the sediment transport direction is mainly towards the north-east, whereas in the second area, the direction is mainly towards the west–south-west. The general characteristics of the talus breccias (e.g., facies and morphology) suggest a rock glacier origin for these deposits (Giraudi, 2003; Kirkbride & Brazier, 1995). The deposition of Subsynthem A occurred during the Early to Middle Pleistocene.

4.3.2 | Subsynthem B

Subsynthem B consists of alluvial fans and debris-fan breccias comprising facies associations F1, F2, and F3 (Figure 4) that unconformably overlie both the Subsynthem A deposits and the pre-Quaternary bedrock. The basal surface (unconformity S2) consists of a marked angular unconformity (Figure 8a). Subsynthem B's thickness is estimated as a few tens of metres and crops out widely in the Dukati subbasin. Smaller exposures have also been recognized in the Tragjas subbasin. In the Dukati subbasin, Subsynthem B consists of a deactivated alluvial fan with its apex near the Dukati village area and a sediment transport direction towards the north-west. Here, the recognized conglomerate facies are strongly related to facies association F1. These deposits pass basinward to facies association F3 deposits through an eteropic contact (Figure 3b). This lateral transition is characterized by a marked decrease in the size and abundance of the conglomerate clasts. In this portion of the basin, the occurrence of sandy facies increases, and as a result, the conglomerate facies are organized as isolated channelized bodies. Seaward, the occurrence of bioturbated sandstones containing trace fossils of *P. surlyki* (Dam, 1990) indicates a marine influence. In the Tragjas subbasin, between the Tragjas and Radhimë localities, the unit consists of a series of coalescing fan breccias, forming a bajada, which retains a preserved palaeo-apex connected to small gullies incised in the local bedrock (Figure 9a). The

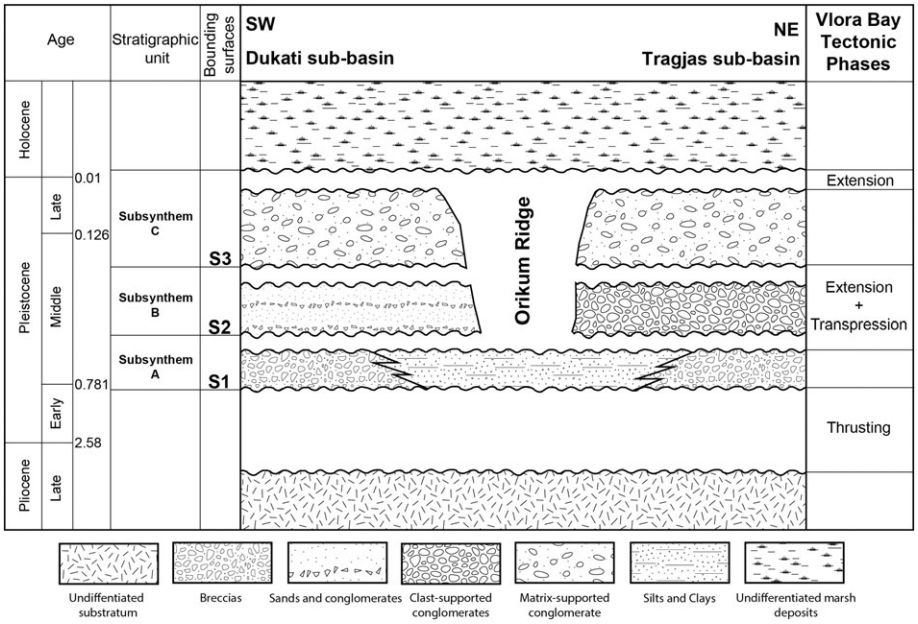

FIGURE 7 Chronostratigraphic diagram showing the distribution of the recognized Pleistocene units through the Vlora Basin. Main tectonic events are indicated

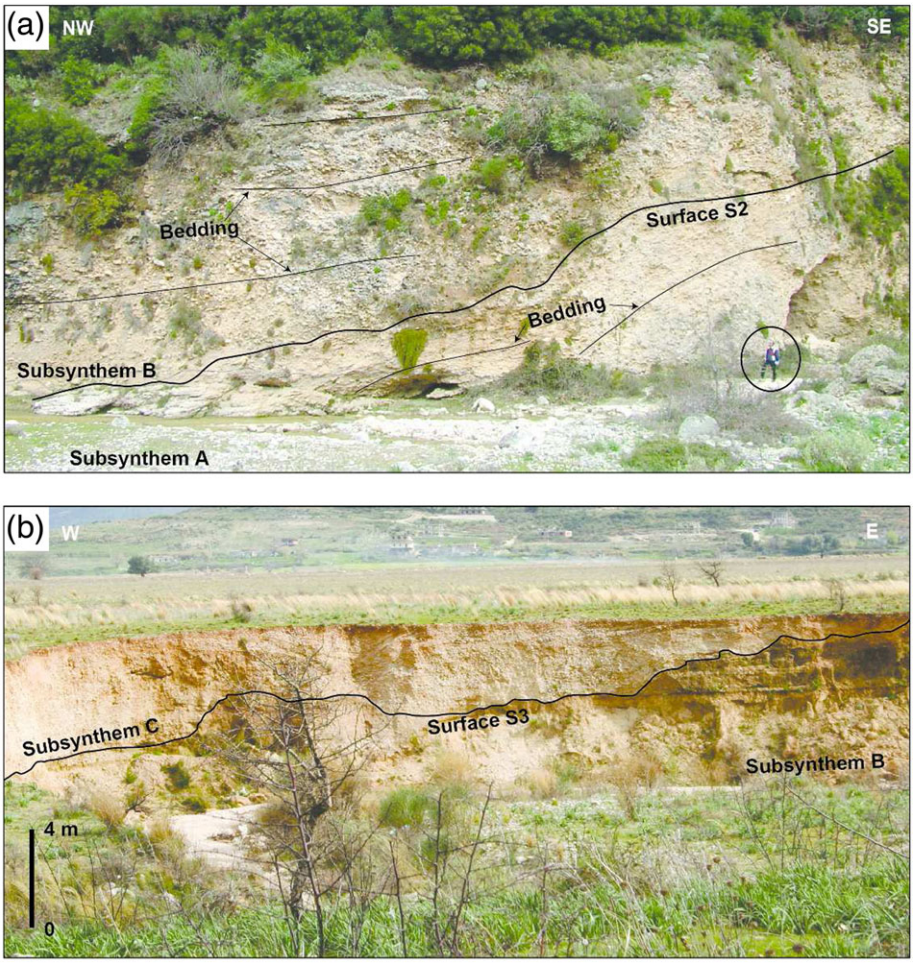

FIGURE 8 Vlora Basin sequence boundaries recognized in the Dukati subbasin sector. (a) The surface S2 consists of an angular unconformity separating the Subsynthems A and B. Note the marked bedding attitude variation between the two conglomeratic successions separated by the stratigraphic discontinuity; (b) the surface S3 consists of a disconformity separating the Subsynthems B and C [Colour figure can be viewed at wileyonlinelibrary.com]

deposits are exclusively related to facies association F2. Fan breccias consist of some metres-thick breccia bodies showing reverse gradation (Facies Bcc; Table 1). One of the best exposed examples is preserved on the ridge hosting the Rarreci village (Figure 9b). In this locality, conglomerate and breccia deposits related to facies associations F2 and F3 crop out. The described fan, which gently slopes seawards, shows a cone apex located at 120 m a.s.l., and the outer portion, which corresponds to the actual coastline, is located at 23 m a.s.l. The deposition of Subsystem B and the formation of the unconformity S2 can probably be dated to the Middle Pleistocene, as a result of several glacial lowstands that occurred in the Mediterranean area (Hughes, Woodward, & Gibbard, 2006; Ridente & Trincardi, 2002). Uncertainty in constraints of the precise age of this subsynthem is mainly due to lack of suitable datable horizons. The concurrence of an intense glacial period may have favoured the production of the large amount of sediments recorded in the considered subbasin during the deposition of Subsynthem B.

4.3.3 | Subsynthem C

Subsynthem C consists of alluvial plain sediments that disconformably overlie Subsynthem B (Figure 8b). The Subsynthem C succession is discontinuously exposed within several incised gullies located on the north-western side of the Dukati subbasin and on the south-western side of the Tragjas subbasin (Figure 2). Structureless or horizontally bedded reddish matrix-supported conglomerates alternating with reddish- or yellowish-coloured silty-sand palaeosoils belonging to facies association F4 are the main deposits characterizing Subsynthem C (Table 2). The basal unconformity S3 consists of a marked erosional surface cutting through the conglomerates of the underlying subsynthem (Figure 2). Unlike the previous subsynthems, this stratigraphic unit was deposited during postglacial climate conditions. The climatic change is demonstrated by the occurrence of reddish palaeosoils, which are indicative of semiarid to arid conditions. Reddish palaeosoil-rich units were widespread during the Middle to Late Pleistocene in the peri-Adriatic area (Giannandrea, 2003, 2009; Lazzari & Pieri, 2002; Sabato, Tropeano, & Pieri, 2004), and Subsynthem C deposits can be attributed to this period.

5 | GEOPHYSICAL SURVEY

A geoelectrical survey was performed along three profiles to better investigate the deep structure of the Dukati subbasin (see the ERT

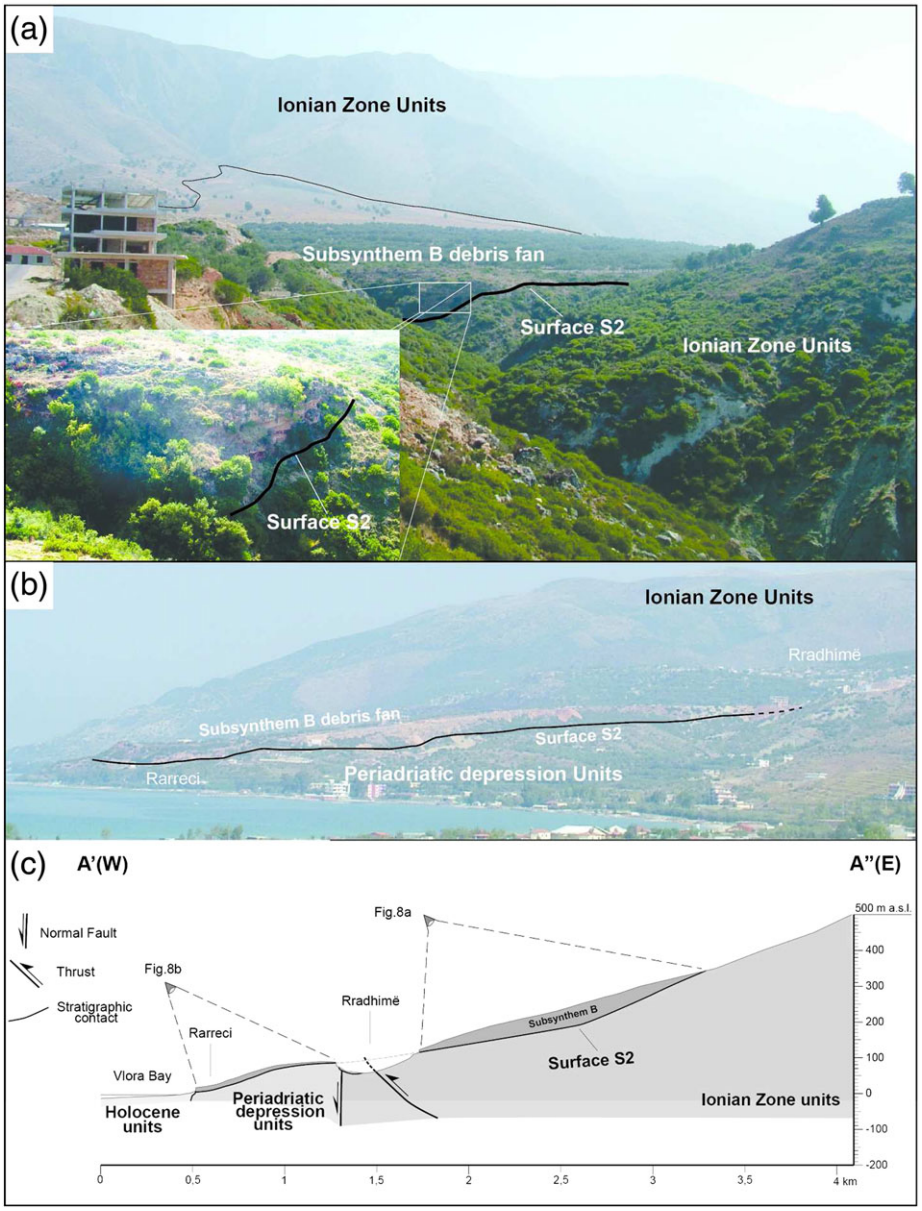

FIGURE 9 Vlora Basin sequence boundaries recognized in the Tragjas subbasin sector. (a) Surface S2 cropping out in the Rarreci/Radhimë area. The surface separate the Subsynthem B debris fan deposits from the underlying pre-Pleistocene substratum; (b) detail of the recognized surface; (c) panorama view of the surface S2 recognized in the Rarreci/Radhimë area, seen from the South; (d) cross-section (A′-A″) through the Tragjas subbasin and Rarreci fan delta (see the location in Figure 2). Vertical scale exaggeration [Colour figure can be viewed at wileyonlinelibrary.com]

profiles traces in Figure 2). ERT profiles were designed to intersect the main basin-bounding tectonic structures at right angles. Profiles W and N are located along the south-western border of the subbasin, whereas Profile E is located on the north-eastern side and intercepts the western side of Orikum Ridge (Figure 10).

Figure 10a shows the resistivity cross-sectional models obtained along the three profiles. The three models display great mutual consistency in terms of both the evaluated resistivity values and the lateral geometric continuity. Laboratory and in situ measurements have shown that the electrical resistivity depends on the grain size: the smaller the grain size, the larger the saturation index and therefore the smaller the electrical resistivity (Schon, 2004). This means that resistivity data can be used as a proxy for sediment grain size (Giocoli et al., 2008; Hickin, Kerr, Barchyn, & Paulen, 2009), which can be explained with the typical depositional criteria. In particular, following Hickin et al. (2009), we can correlate resistivity values with the Vlora Basin rock types grain size categorizing them into fine-grained (<400 ohm-m), sand-size (400–800 ohm-m), and gravel-sized (>800 ohm-m) sediments. Similar associations were made by other authors (e.g., Bersezio, Giudici, & Mele, 2007).

In general, we observe that the highest resistivity values (coarse-grained sediments) are quite common in the Profiles W and E. On the contrary, low resistivity values (fine-grained sediments) are more common in the Profile N. This fits well with outcrop observations in which coarse-grained material is found in proximal areas, whereas fine-grained material is found in distal areas of the basin. In the Dukati subbasin subsurface, the resistivity generally decreases with depth (Figure 10a). The main subhorizontal or wave-shaped resistivity

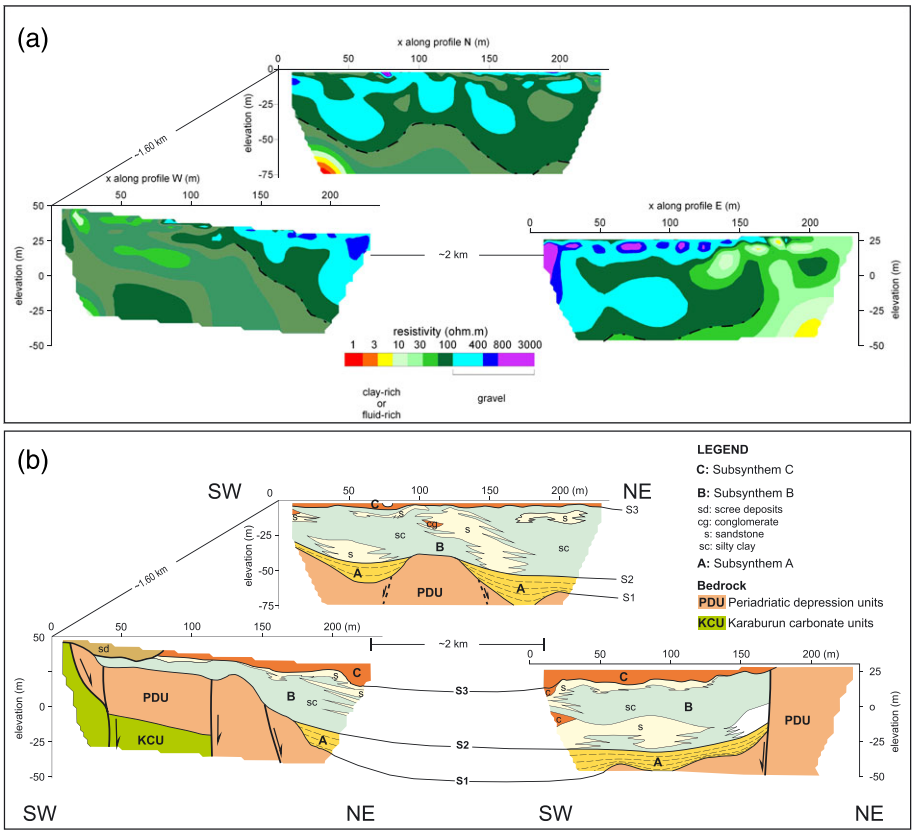

FIGURE 10 (a) Resistivity cross-sections acquired in the Dukati subbasin (see Figure 2 for location). (b) Interpretation outlying the main discontinuities and geometries recognized in the Dukati subbasin (see text for explanation) [Colour figure can be viewed at wileyonlinelibrary.com]

contrast, which occurs, on average, between 25 and 50 m below the topographic surface, is interpreted as the Vlora Basin succession basal unconformity S1. Vertically or obliquely oriented resistivity contrasts are generally interpreted as tectonic discontinuities.

By merging general subsurface observations and outcrop data, a detailed geological interpretation of the three resistivity models is obtained (Figure 10b).

Profile W shows the details of the south-western side of the Dukati subbasin. It displays a series of down-stepping normal faults cutting through the pre-Quaternary substratum represented by the KCUs and the overlying PDUs. Above this bedrock, approximately 75 m of Quaternary sediments fill the resulting tectonic depression. According to the outcrop observations, extensional faults are interpreted to cut through the Subsynthem A deposits. The profile shows a clear basal unconformity (surface S1), whereas intra-Quaternary discontinuities are less evident. High resistivity values, observable in the middle portion and at the top of the Quaternary succession, are attributed to the Subsynthem A and B coarse-grained deposits. The low resistivity values found immediately above the surface S1 are interpreted as the Subsynthem A deposits. The measured low resistivity values recognized in the western side of the profile can be in part attributed to the occurrence of highly fractured, probably water-saturated, limestones and in part to presence of fine-grained deposits, which represent the distal counterpart of the outcropping Subsynthem A breccias.

Profile E shows details of the eastern side of the Dukati subbasin corresponding to Orikum Ridge. The basin margin corresponds to a south-west-dipping discontinuity interpreted as a normal fault. In the correspondence of the Subsynthem B, portions of the section showing high resistivity values are interpreted as gravel or sand bodies isolated in finer sediments. At the top of the succession, the alignment of very bright spots evidences the occurrence of gravel deposits pertaining to Subsynthem C.

Profile N, which runs roughly parallel to Profile W, clearly shows the stratigraphic organization of the considered Quaternary deposits. At their base, the pre-Quaternary substratum results are segmented into a series of highs and lows interpreted as alternating horst and graben, respectively. According to the outcrop data, the Subsynthem A deposits are interpreted as offset by the bounding extensional faults. In the middle portion of the Quaternary succession, the patchy rounded portions, which show high resistivity values, are interpreted as isolated channelized conglomerates included in finer sediments.

6 | PLEISTOCENE TECTONICS

In the Vlora Bay area, a series of extensional and transcurrent Pleistocene faults overprinted contractional structures related to the building of the Albanian chain-foredeep–foreland system during the Cenozoic. These younger structures were responsible for the continuous creation and destruction of accommodation space recorded throughout the Vlora Basin stratigraphy. In addition, they importantly contributed to the production of the abundant sediments accumulated during the Pleistocene in the Dukati and Trajas subbasins.

Based on cross-cutting relationships, the older generation of faults affecting the Vlora Basin deposits are considered as a series of roughly parallel, north-west–south-east- and north–south-trending extensional faults. Along the eastern border of the Vlora Basin, these structures produced a series of blocks down-stepping to the north-east, observable in both the outcrop and geoelectrical profile ERT W (Figure 10). In the middle portion of the basin, according to outcrop and subsurface data (see ERTs N and E in the Figure 10), extensional faults were responsible for the dissection of surface S1, the creation of the horst- and graben-like geometries, and the deformation of Subsynthem A deposits. Orikum Ridge is the main morpho-structural expression produced during this extensional tectonic stage. West of the Radhimë area, east-dipping, north–south-trending normal faults, which affect the Meso-Cenozoic bedrock, are well-preserved morphological steps along the slope profile (Figure 11a). North of Tragjas village, the mentioned extensional structures are responsible for the deformation of the Subsynthem A deposits, which actually dip 45° towards the east (Figure 2).

The second generation of Quaternary faults delimits the south-western border of the Vlora Basin. These faults, which are well preserved in the Karaburun carbonate lithologies, are part of a narrow but 15-km-long shear zone that is referred to in this paper as the

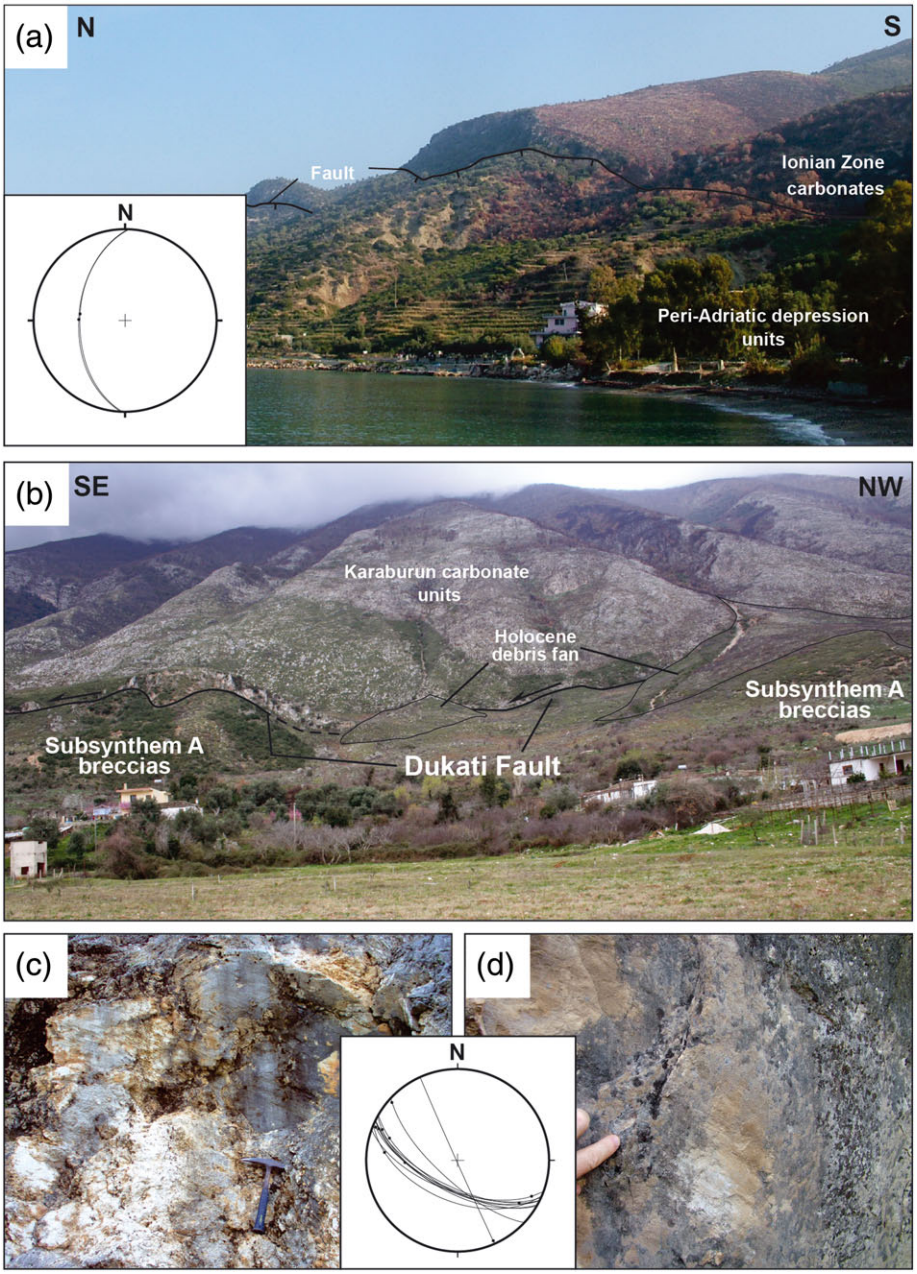

FIGURE 11 (a) Panorama view of the N–S trending fault plane, recognized in the Radhimë area. This west-dipping structure shows at the footwall the Mesozoic Ionian bedrock and, at the hanging wall, the Pliocene Peri-Adriatic Depression deposits; in the field, the structure is made obvious by the steep fault scarp profile; (b) panorama view of the Dukati Fault observable west of Dukati i Ri village; based on the recognition of oblique striae and steps, this structure is interpreted as a left-lateral transpressive fault; (c) particulars of the Dukati Fault plane; note the slickensides and the fault breccia still preserved on the fault plane. (d) Fault steps recognized on the Dukati Fault plane [Colour figure can be viewed at wileyonlinelibrary.com]

Dukati Fault Zone. The Dukati Fault Zone is a major reactivated structure that is quite easy to follow in the field from Dukati i Ri Village to the Adriatic Sea (Figure 2). During the Cenozoic, this fault consisted of a major north-west–south-east-oriented, south-west-dipping, backthrust superimposing the Sazani Zone carbonates on the Peri-Adriatic foredeep unit (Roure, 2008). During the Pleistocene, the structure was reactivated as a left-lateral transpressive fault. The Dukati Fault Zone consists of a main fault plane and a series of associated mesoscale strike-slip faults (Figure 11b). The transpressive kinematism of the structure is deduced in the analysis of slickensides and calcite steps (Figure 11c,d). Locally, the main fault plane tends to assume a vertical attitude and, in some cases, weakly dips towards the north-east. The Pleistocene activity of the structure may be deduced from the ages of the younger deposits involved in the deformation, which consist of conglomerates and breccias belonging to Subsynthems A and B (Figures 2 and 11a), and by the cross-cutting relationships with the previously described extensional faults, which abruptly end against the Dukati Fault Zone (Figure 2).

The younger tectonic structures recognized in the Vlora Basin consist of a series of east–west- and south-west–north-east-oriented normal faults that postdate the Subsynthem C deposits (Figure 2). Well-exposed normal fault planes are recognized immediately south of Dukati i Ri village (Figure 12a). Here, these structures are in contact with the Pliocene deposits belonging to the Vlora Basin bedrock and reddish deposits belonging to Subsynthem C. Well-preserved slickensides are recognized above the fault plane (Figure 12c). The estimated fault offset values vary from metres to a few centimetres (Figure 12c), and their preferential orientations are displayed in the plots of Figure 12d. In the plan view, these faults locally display a series of anastomizing branches. Commonly, these structures cross-cut the older, previously described faults, and some have been recognized between the Tragjas and Dukati area cutting through Orikum Ridge and diverting the original course of the Dukati River (Figure 2).

7 | TECTONOSTRATIGRAPHIC EVOLUTION OF THE VLORA BASIN

Detailed sedimentological and stratigraphic analyses performed on the Quaternary deposits cropping out along the Vlora Bay, which were supported by structural and geophysical data, reveal significant complexity in the evolution of the Vlora Basin. Based on the collected data, an evolutionary palaeogeographical model showing the depositional history of the basin and the main tectonic phases is proposed (Figure 13). Our reconstructions take into account the time span between the latest contractional stages that occurred during the Pliocene and the present-day conditions.

The Vlora Basin-fill history starts with the development of a triangle zone between the Sazani and Ionian zones and the concomitant emersion of the Albano-Hellenic thrust belt front–foredeep–foreland system at the Pliocene–Early Pleistocene transition (Roure et al., 2004; Velaj, 2011; Figure 13a). At this time, because of the contractional deformation, the Karaburun Peninsula was folded, uplifted, and backthrusted onto the PDUs, giving rise to the south-western border of Vlora Bay (Argnani, 2013). On the opposite side, the deformed Ionian Zone represented the north-eastern flanks of Vlora Bay (Velaj, 2011). The creation of the surface S1 can be traced back to this period (Figure 7). Along the emerged, steeply dipping flanks of the basin, the

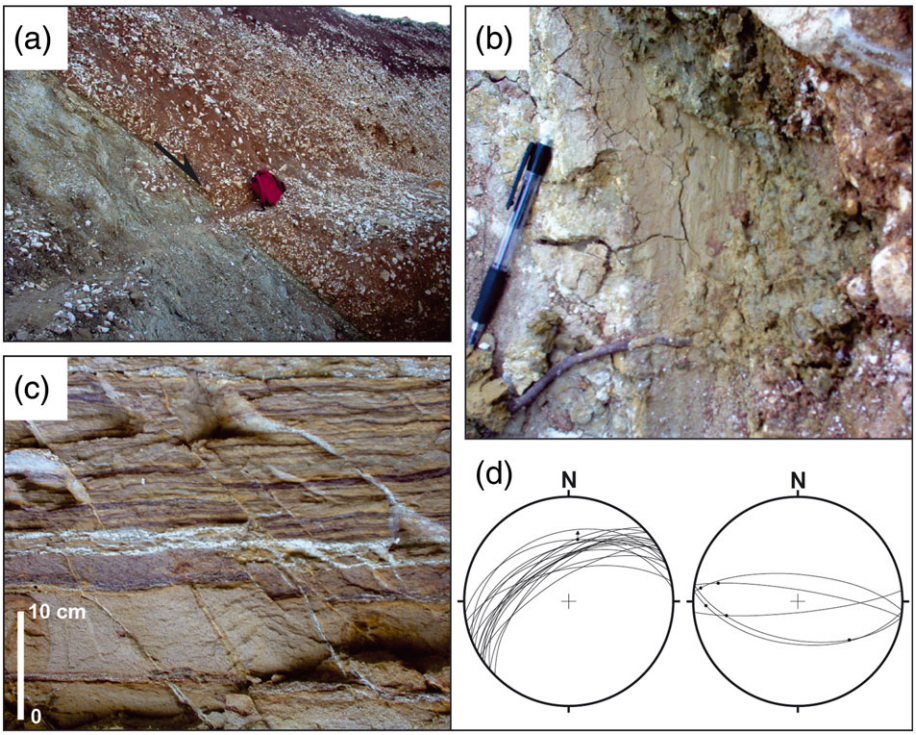

FIGURE 12 (a) Extensional faults recognized immediately south of the Dukat i Ri village, displaying red-matrix breccias (Subsynthem C) at the hanging wall and Pliocene sandy–clay alternation at the footwall; (b) particulars of the fault plane, note the dip–slip orientation of the slickensides; (c) minor extensional fault plane recognized in the Dukat i Ri village; (d) stereoplots showing the preferential orientations of the described extensional faults [Colour figure can be viewed at wileyonlinelibrary.com]

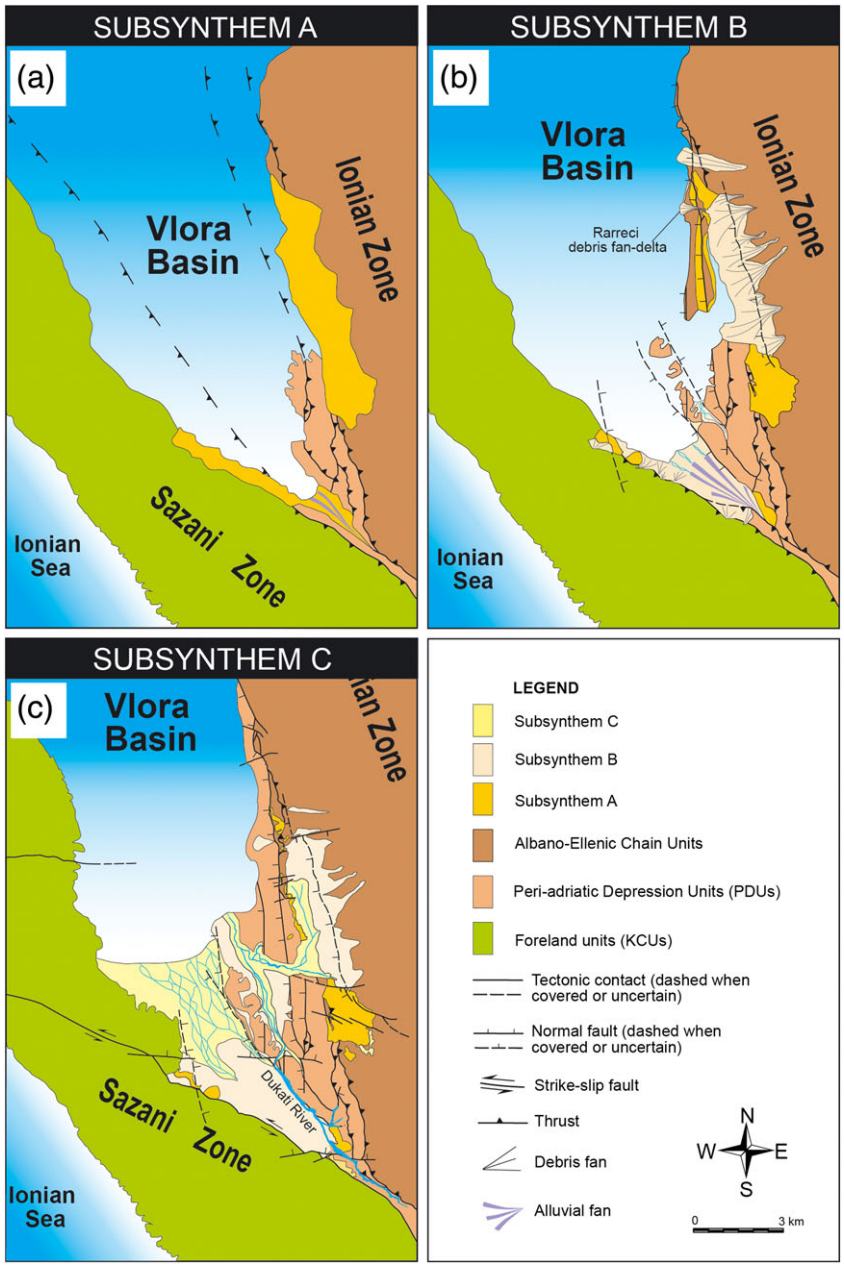

FIGURE 13 Tectonostratigraphic evolutionary model of the Vlora Basin during the deposition of the recognized subsynthems. The Quaternary basin fill history of the Vlora Basin can be summarized in three main stages (see text for explanation) [Colour figure can be viewed at wileyonlinelibrary.com]

Subsynthem A sediments, represented by coalescing fan-shaped scree deposits, mainly accumulated at the base of slopes, forming thick carbonate talus breccia bodies. In the submerged portion of the basin, fine-grained sedimentation occurred, as demonstrated by the low-resistivity unit recognized in ERT W (Figure 10).

The deposition of Subsynthem A was followed by an intense uplift phase, which led to important physiographic changes in the Vlora basin during the Middle Pleistocene (Figure 13b). In response, extensional tectonics developed to accommodate this deformation, and the basin bottom was modelled in a series of alternating horst and graben. Another consequence was the retreat of the sea towards its present-day position. The emersion of Orikum Ridge in the middle portion of the basin is related to this period, and its growth gave rise to two separated depocentres represented by the Dukati and Tragjas subbasins. Along the basin margins, a series of north-west–south-east- and north–south-trending extensional faults led to the down-stepping configuration that are still recognizable today in the subsurface (Figure 10b) or outcrops along the flanks of the subbasins (Figure 11). As a result of extensional tectonics, the carbonate talus breccia related to Subsynthem A was faulted and, in some cases, tilted and detached from the original substratum. The creation of the unconformity S2 and the deposition of Subsynthem B occurred along with or immediately followed this tectonic stage. In the Dukati subbasin, the growth of the Dukati alluvial fan system proceeded towards the north-west according to the progressive retreat of the sea in the same direction. Laterally, a series of debris fans fed by the KCUs also contributed to filling up the available accommodation space (Figure 13b). In the Tragjas subbasin, the general uplift of the area led to the deposition of the bajada-type debris fans along the slope of the External Albanides chain front and the Rarreci debris-fan delta (Figure 9).

During the Middle–Late Pleistocene, this period of sedimentation was once again interrupted by a new tectonic phase that resulted in the reactivation of the Dukati Fault Zone as a transpressional fault (Figure 13c). This phase caused an ultimate uplift of the Karaburun

Peninsula area, the deformation of the Subsynthem B deposits, and a further shift of the coastline towards the north-east. The consequent sea-level drop led to the development of the erosional surface S3 and the onset of a wide alluvial plain related to Subsynthem C, which is recorded in both the Dukati and Tragjas subbasins.

The latest tectonic evolution of the Vlora Basin is related to the activation of the east–west-oriented normal faults during the Late Pleistocene (Figure 13c). This tectonic phase caused the deformation of the Vlora Basin and its definitive deactivation.

Currently, the Vlora Basin deposits are partially covered by Holocene to present-day deposits outcropping along the Vlora Bay shore area (Figure 2). They are separated by a basal disconformity that formed during a period of sea-level fall recorded in the peri-Adriatic area (Amorosi, Maselli, & Trincardi, 2016; Cattaneo, Trincardi, Asioli, & Correggiari, 2007; Pellegrini et al., 2015).

8 | CONCLUSIONS

Based on a multidisciplinary approach that takes into account sedimentological, structural, and geophysical observations, a stratigraphic subdivision and evolutionary tectonostratigraphic model are proposed for the Quaternary deposits filling the Vlora Basin. The occurrence of two minor unconformities, recognized in outcrops and in the subsurface by means of a geoelectrical survey, allows the Vlora Basin infill to be subdivided into three subsynthems. The oldest, Subsynthem A, constitutes calcareous talus breccias passing laterally in the subsurface to silty clayey sediments. Subsynthem B consists of alluvial to fan fringe marine systems and fan breccias. Subsynthem C consists of reddish alluvial sediments in a matrix. The entire succession records a general increase in the temperature during the Quaternary, from the cold climate of Subsynthems A and B to the semiarid to arid climate of Subsynthem C. In the proposed model, the tectonic activity continuously modified the basin geometry, producing differential accommodation space for the sediments that were subdivided. We suggest that, during the Quaternary, the basin was strongly controlled by contractional, transpressional, and extensional tectonics. In particular, tectonic activity exerted important allogenic control over the creation of the main unconformities and producing sediments in the Vlora Basin. Climate and eustasy may have also played an important role in the sedimentary supply. During the Middle Pleistocene, the growth of Orikum Ridge divided the basin into two portions, represented by the Dukati and Tragjas subbasins, which show slightly different geological evolutions. The main difference is recorded by the sediments of Subsynthem B, which consist of alluvial to fan fringe marine systems in the Dukati Basin and coalescing fan breccias in the Tragjas subbasin.

ACKNOWLEDGEMENTS

We wish to thank Prof. Marcello Schiattarella (Universita' degli Studi della Basilicata) for his suggestions. We would also thank F. Roure and the three anonymous reviewers for their critical review and suggestions leading to the improvement of the paper. This study benefited from the funding supported by the CISM project and by Fondi di Ateneo RIL 2011 and 2013 (Universita' degli Studi della Basilicata) granted to Paolo Giannandrea.

REFERENCES

Aliaj, S. H. (1987). On some fundamental aspects of the structural evolution of the outer zone of the Albanides. *Bulletin of Geological Science*, *4*, 2–11.

Aliaj, S. (2006). The Albanian orogeny: convergence zone between Eurasia and the Adria microplate. In N. Pinter, G. Grenerczy, J. Weber, S. Stein, & D. Medak (Eds.), *The Adria microplate: GPS geodesy, tectonics and hazards* (Vol. 61 *Nato Science Series, IV, Earth and Environmental Science*) (pp. 133–149). Dordrecht: Springer.

Amorosi, A., Maselli, V., & Trincardi, F. (2016). Onshore to offshore anatomy of a late Quaternary source-to-sink system (Po Plain–Adriatic Sea, Italy). *Earth-Science Reviews*, *153*, 212–237.

Argnani, A. (2013). The influence of Mesozoic palaeogeography on the variations in structural style along the front of the Albanide thrust-and-fold belt. *Italian Journal of Geoscience*, *132*(2), 175–185.

Bersezio, R., Giudici, M., & Mele, M. (2007). Combining sedimentological and geophysical data for high-resolution 3-D mapping of fluvial architectural elements in the Quaternary Po plain (Italy). *Sedimentary Geology*, *202*, 230–248.

Besley, B. M., & Turner, P. (1983). Origin of red beds in a moist tropical climate (Etruria Formation, Upper Carboniferous, UK). In R. C. L. Wilson (Ed.), *Residual deposits* (Vol. 11) (pp. 131–147). London: Geological Society, Special Publications.

Blair, T. C. (1987). Sedimentary processes, vertical stratification sequences, and geomorphology of the Roaring River alluvial fan, Rocky Mountain National Park, Colorado. *Journal of Sedimentary Petrolology*, *58*, 623–636.

Blair, T. C., & McPherson, J. G. (1994). Alluvial fan processes and forms. In A. D. Abrahams, & A. J. Parsons (Eds.), *Geomorphology of desert environments* (pp. 354–402). London: Chapman and Hall.

Bosellini, A. (2002). Dinosaurs "re-write" the geodynamics of the eastern Mediterranean and the paleogeography of the Apulia Platform. *Earth-Science Reviews*, *59*, 211–234.

Carcaillet, J., Mugnier, J. L., Koçi, R., & Jouanne, F. (2009). Uplift and active tectonics of southern Albania inferred from incision of alluvial terraces. *Quaternary Research*, *71*, 465–476.

Cattaneo, A., Trincardi, F., Asioli, A., & Correggiari, A. (2007). The Western Adriatic shelf clinoform: Energy-limited bottomset. *Continental Shelf Research*, *27*, 506–525.

Chang, K. H. (1975). Unconformity-bounded stratigraphic units. *Geological Society of America Bulletin*, *86*, 1544–1552.

Channel, J. E. T., D'Argenio, B., & Horvath, F. (1979). Adria, the African promontory, in Mesozoic Mediterranean Palaeogeography. *Earth-Science Reviews*, *15*, 213–292.

D'Agostino, N., Avallone, A., Cheloni, D., D'Anastasio, E., Mantenuto, S., & Selvaggi, G. (2008). Active tectonics of the Adriatic region from GPS and earthquake slip vectors. *Journal of Geophysical Research*, *113*. B12413. DOI: https://doi.org/org/10.1029/2008JB005860

Dam, G. (1990). Palaeoenvironmental significance of trace fossils from the shallow marine Lower Jurassic Neill Klinter Formation, East Greenland. *Palaeogeography, Palaeoclimatology, Palaeoecology*, *79*, 221–248.

Dercourt, J., Zonenshain, L. P., Ricou, L. E., Kazmin, V. G., Pichon, X. L., Knipper, A. L., … Biju-Duval, B. (1986). Geological evolution of the Tethys belt from the Atlantic to the Pamirs since the Lias. *Tectonophysics*, *123*, 241–315.

Dercourt, J., Ricou, L. E., & Vrielynck, B. (1993). Atlas Tethys palaeoenvironmental maps. Beicip-Franlab.

Doglioni, C., Mongelli, F., & Pieri, P. (1994). The Puglia uplift (SE Italy): An anomaly in the foreland of the Apenninic subduction due to buckling of a thick continental lithosphere. *Tectonics*, *13*, 1309–1321.

Frasheri, A., Nishani, P., Bushati, S., & Hyseni, A. (1996). Relationship between tectonic zone of the Albanides, based on results of geophysical studies. In P. A. Ziegler, & F. Horwath (Eds.), *Peri-Tethys Memoir 2: Structure and prospects of Alpine basins and forelands* (Vol. 170) (pp. 485–511). Paris: Mem. Musee Hist. Nat.

Fürsich, F. T., Wilmsen, M., & Seyed-Emami, K. (2006). Ichnology of lower Jurassic beach deposits in the Shemshak Formation at Shahmirzad, southeastern Alborz Mountains, Iran. *Facies*, *52*, 599–610.

Gealey, W. K. (1988). Plate tectonic evolution of the Mediterranean-Middle East region. *Tectonophysics*, *155*, 285–306.

Giannandrea, P. (2003). Analisi sedimentologica del Sintema di M. Sirico (parte alta della successione del Bacino dell'Ofanto), Appennino Meridionale, Basilicata. *Il Quaternario*, *16*, 269–277.

Giannandrea, P. (2009). Evoluzione sedimentaria della successione alluvionale e lacustre quaternaria del Bacino di Venosa (Italia meridionale). *Il Quaternario*, *22*, 269–290.

Giannandrea, P., Marino, M., Romeo, M., & Schiattarella, M. (2014). Pliocene to Quaternary evolution of the Ofanto Basin in southern Italy: An approach based on the unconformity-bounded stratigraphic units. *Italian Journal of Geoscience*, *133*(1), 27–44.

Giocoli, A., Magri', C., Vannoli, P., Piscitelli, S., Rizzo, E., Siniscalchi, A., … Di Nocera, S. (2008). Electrical resistivity tomography investigations in the Ufita Valley (Southern Italy). *Annales de Geophysique*, *51*, 213–223.

Giraudi, C. (2003). Middle Pleistocene to Holocene Apennine glaciations (Italy). *Il Quaternario*, *16*, 37–48.

Gloppen, T. G., & Steel, R. J. (1981). The deposits, internal structure and geometry in six alluvial fan delta bodies (Devonian-Norway)—A study case in the significance of bedding sequence in conglomerates. In F. G. Ethridge, & R. M. Flores (Eds.), *Recent and ancient non-marine depositional environments: Models for exploration* (Vol. 31) (pp. 49–69). Tulsa: SEPM Special Publication.

Hickin, A. S., Kerr, B., Barchyn, T. E., & Paulen, R. C. (2009). Using ground-penetrating radar and capacitively coupled resistivity to investigate 3-D fluvial architecture and grain-size distribution of a gravel floodplain in northeast British Columbia, Canada. *Journal of Sedimentary Research*, *79*(6), 457–477.

Hughes, P. D., Woodward, J. C., & Gibbard, P. L. (2006). Quaternary glacial history of the Mediterranean mountains. *Progress in Physical Geography*, *30*, 334–364.

ISPGJ-IGJN (1982). *Geology of Albania*. Albania: Tirana.

ISPGJ-IGJN (1983). *Geological map of Albania*. Albania: Tirana. Scale 1:200,000

Jouanne, F., Mugnier, J. L., Koci, R., Bushati, S., Matev, K., Kuka, N., … Duni, L. (2012). GPS constraints on current tectonics of Albania. *Tectonophysics*, *554–557*, 50–62.

Kirkbride, M., & Brazier, V. (1995). On the sensitivity of Holocene talus-derived rock glaciers to climate change in the Ben Ohau Range, New Zealand. *Journal of Quaternary Science*, *10*, 353–365.

Lacombe, O., Malandain, J., Vilasi, N., Amrouch, K., & Roure, F. (2009). From paleostresses to paleoburial in fold–thrust belts: Preliminary results from calcite twin analysis in the Outer Albanides. *Tectonophysics*, *475*, 128–141.

Lazzari, M., & Pieri, P. (2002). Modello stratigrafico-deposizionale della successione regressiva infrapleistocenica della Fossa Bradanica nell'area compresa tra Lavello, Genzano e Spinazzola. *Memorie della Societa Geologica Italiana*, *57*(1), 231–237.

Loiacono, F., Giannandrea, P., Palladino, G., Siniscalchi, A., Dallarche, F., Magrì, C., & Piras, G. (2008). Studio tettono-stratigrafico dell'area emersa e sommersa sottesa dal Golfo di Valona. In A. Tursi, & C. Corselli (Eds.), *CISM Project* (Vol. 1*Relazione Finale*) (pp. 53–73).

Loiacono, F., De Marco, A., Dicoladonato, G., Gadaleta, M. V., & Durmischi, C. (2011). Recent sedimentation in the Vlora Gulf: Grain size and mineralogical analyses from some cores in a EW transect. *Journal of Coastal Research*, *58*, 17–25.

Loke, M. H., & Barker, R. D. (1996). Rapid least-squares inversion of apparent resistivity pseudosections using a quasi-Newton method. *Geophysical Prospecting*, *44*, 131–152.

Mack, G. H., & Madoff, R. D. (2005). A test of models of fluvial architecture and palaeosol development: Camp Rice Formation (Upper Pliocene–Lower Pleistocene) southern Rio Grande rift, New Mexico, USA. *Sedimentology*, *52*, 191–211.

Meço, S., & Aliaj, S. (2000). *Geology of Albania. Beitraege zur Regionalen Geologie der Erde*. Berlin: Gebrüder Borntraeger.

Miall, A. D. (1992). Alluvial deposits. In R. G. Walker, & M. P. James (Eds.), *Facies models: Response to sea-level change* (pp. 119–142). Newfoundland, Canada: Geological Association of Canada.

Miall, A. D. (1996). *The geology of fluvial deposits: Sedimentary facies, basin analysis and petroleum geology*. New York: Springer.

Palladino, G. (2011). Tectonic and eustatic controls on Pliocene accommodation space along the front of the southern Apennine thrust-belt (Basilicata, southern Italy). *Basin Research*, *23*, 591–614. https://doi.org/10.1111/j.1365-2117.2011.00503.x

Papa, A., & Kondo, A. (1968). Reflections about the Sazani zone and its transition to the Ionian zone. *Bulletin Tirana University Natural Science*, *2*, 44–47.

Paschinger, H. (1950). Morphologische Ergebnisse einer Analyse der Höttinger Brekzie bei Innsbruck. *Schlern Schriften*, *75*, 7–86.

Pellegrini, C., Maselli, V., Cattaneo, A., Piva, A., Ceregato, A., & Trincardi, F. (2015). Anatomy of a compound delta from the post-glacial transgressive record in the Adriatic Sea. *Marine Geology*, *362*, 43–59.

Penck, A. (1921). *Die Höttinger Breccie und die Inntalterrasse nördlich Innsbruck*. Berlin: Verlag der Akademie der Wissenschaften.

Pierson, T. C. (1980). Erosion and deposition by debris flows at Mount Thomas, North Canterbury, New Zealand. *Earth Surface Processes*, *5*, 227–247.

Pinter, N., Grenerczy, G., Weber, J., Stein, S., & Medak, D. (2006). *The Adria microplate: GPS geodesy, tectonics and hazards* (Vol. 61) *NATO Science Series, IV, Earth and Environmental Science*. Dordrecht: Springer.

Reid, I., & Frostick, L. E. (1984). Particle interaction and its effect on the thresholds of initial and final bedload motion in coarse alluvial channels. In E. H. Koster, & R. J. Steel (Eds.), *Sedimentology of gravels and conglomerates* (Vol. 10 *Can. Soc. Pet. Geol. Mem*) (pp. 61–68).

Ridente, D., & Trincardi, F. (2002). Eustatic and tectonic control on deposition and lateral variability of Quaternary regressive sequences in the Adriatic basin (Italy). *Marine Geology*, *184*, 273–293.

Robertson, A., & Shallo, M. (2000). Mesozoic–Tertiary tectonic evolution of Albania in its regional Eastern Mediterranean context. *Tectonophysics*, *316*, 197–254.

Roure, F. (2008). Foreland and hinterland basins: What controls their evolution? *Swiss Journal of Geosciences*, *101*(Supplement 1), S5–S29. https://doi.org/10.1007/s00015-008-1285-x

Roure, F., Prenjasi, E., & Xhafa, Z. (1995). Albania: Petroleum geology of the Albanian thrust belt. AAPG Int. Conference and Exhibition, Nice, Field Trip Notes, Trip # 7.

Roure, F., Nazaj, S., Mushka, K., Fili, I., Cadet, J. P., & Bonneau, M. (2004). Kinematic evolution and petroleum systems—an appraisal of the Outer Albanides. In K. R. McClay (Ed.), *Thrust tectonics and hydrocarbon systems* (Vol. 82 *AAPG Mem*) (pp. 474–493).

Sabato, L., Tropeano, M., & Pieri, P. (2004). Problemi di cartografia geologica relativa ai depositi del F° 471 "Irsina". Il Conglomerato di Irsina: mito o realtà? *Il Quaternario*, *17*, 391–404.

Salvador, A. (1987). Unconformity-bounded stratigraphic units. *Geological Society American Bulletin*, *98*, 232–237.

Salvador, A. (1994). International stratigraphic guide. International Union of Geological Sciences, Trondheim, Norway, and Geological Society of America, Boulder.

Sanders, D., Ostermann, M., & Kramers, J. (2009). Quaternary carbonate-rocky talus slope successions (Eastern Alps, Austria): Sedimentary facies and facies architecture. *Facies*, *55*, 345–373.

Sanders, D., Ostermann, M., & Kramers, J. (2010). Meteoric diagenesis of quaternary carbonate-rocky talus slope successions (Northern Calcareous Alps, Austria). *Facies*, *56*, 27–46.

Savini, A., Corselli, C., Durmishi, C., Markus, S., Morelli, D., & Tessarolo, C. (2011). Geomorphology of the Vlora Gulf Seafloor: Results from multibeam and high-resolution seismic data. *Journal of Coastal Research*, *58*, 6–16.

Schon, J. H. (2004). *Physical properties of rocks: Fundamentals and principles of petrophysics*. Amsterdam: Elsevier.

Sejdini, B., Constantinescu, P., & Piperi, T. (1994). Petroleum exploration in Albania. In B. Popesku (Ed.), *Hydrocarbons of eastern central Europe* (pp. 1–28). Heidelberg: Springer-Verlag.

Smith, G. A. (1986). Coarse-grained nonmarine voicaniclastic sediment: Terminology and depositional process. *Geological Society of America Bulletin*, *97*, 1–10.

Speranza, F., Islami, I., Kissel, C., & Hyseni, A. (1995). Palaeomagnetic evidence for clockwise rotation of the external Albanides. *Earth and Planetary Science Letters*, *129*, 121–134.

Todd, S. P. (1989). Stream-driven, high-density gravelly traction carpets: Possible deposits in the Trabeg Conglomerate Formation, SW Ireland and some theoretical considerations of their origin. *Sedimentology*, *36*, 513–530.

Van Houten, F. B. (1968). Iron oxides in red beds. *Geological Society of America Bulletin*, *79*, 399–416.

Velaj, T. (2011). Tectonic style in Western Albania Thrustbelt and its implication on hydrocarbon exploration. AAPG International Convention and Exhibition, Milan, Italy, October 23–26.

Velaj, T., Davinson, I., Serjani, A., & Alsop, I. (1999). Thrust tectonics and the role of evaporites in the Ionian Zone of the Albanides. *AAPG Bulletin*, *83*, 1408–1425.

Walker, T. R. (1967). Color of recent sediments in tropical Mexico: A contribution to the origin of red beds. *Bulletin Geological Society of America*, *78*, 917–920.

How to cite this article: Palladino G, Giannandrea P, Siniscalchi A, Magri' C, Loiacono F. Quaternary tectonostratigraphic evolution of the Vlora Basin, south-western Albania. *Geological Journal*. 2017;1–18. https://doi.org/10.1002/gj.2992